ORIGINAL ARTICLE

# In vivo and in vitro examination of the functional significances of novel lamin gene mutations in heart failure patients

**N Sylvius, Z T Bilinska, J P Veinot, A Fidzianska, P M Bolongo, S Poon, P McKeown, R A Davies, K-L Chan, A S L Tang, S Dyack, J Grzybowski, W Ruzyllo, H McBride, F Tesson**

*J Med Genet* 2005;**42**:639–647. doi: 10.1136/jmg.2004.023283

See end of article for authors' affiliations

Correspondence to: Dr F Tesson, University of Ottawa Heart Institute, 40 Ruskin Street, Ottawa, Ontario K1Y 4W7, Canada; ftesson@ottawaheart.ca

Received 26 May 2004
Revised 31 January 2005
Accepted 4 February 2005

**Context:** Lamin A/C (*LMNA*) gene variations have been reported in more than one third of genotyped families with dilated cardiomyopathy (DCM). However, the relationship between *LMNA* mutation and the development of DCM is poorly understood.

**Methods and results:** We found that end stage DCM patients carrying *LMNA* mutations displayed either dramatic ultrastructural changes of the cardiomyocyte nucleus (D192G) or nonspecific changes (R541S). Overexpression of the D192G lamin C dramatically increased the size of intranuclear speckles and reduced their number. This phenotype was only partially reversed by coexpression of the D192G and wild type lamin C. Moreover, the D192G mutation precludes insertion of lamin C into the nuclear envelope when co-transfected with the D192G lamin A. By contrast, the R541S phenotype was entirely reversed by coexpression of the R541S and wild type lamin C. As lamin speckle size is known to be correlated with regulation of transcription, we assessed the SUMO1 distribution pattern in the presence of mutated lamin C and showed that D192G lamin C expression totally disrupts the SUMO1 pattern.

**Conclusion:** Our in vivo and in vitro results question the relationship of causality between *LMNA* mutations and the development of heart failure in some DCM patients and therefore, the reliability of genetic counselling. However, *LMNA* mutations producing speckles result not only in nuclear envelope structural damage, but may also lead to the dysregulation of cellular functions controlled by sumoylation, such as transcription, chromosome organisation, and nuclear trafficking.

Dilated cardiomyopathy (DCM) is characterised by dilatation of cardiac chambers and impaired contraction, leading to heart failure or sudden death. Symptoms are highly variable in severity and age of onset. Penetrance has been found to be incomplete and age related in most families. [1–3] DCM appears to be a complex genetic disorder, with 16 genes being implicated in autosomal dominant DCM (OMIM #115200). What is remarkable about DCM is that a variation in one of these genes does not result exclusively in a DCM phenotype. In particular, lamin A/C (*LMNA*) mutations have also been described in at least nine other diseases, including Emery-Dreifuss and other types of muscular dystrophy, lipodystrophy disorders, Charcot-Marie-Tooth disorder type 2, Hutchinson-Gilford progeria syndrome, and restrictive dermopathy (OMIM #150330[4]). We calculated from extensive review of the literature that more than one third of reported DCM genotyped families carry a mutation in *LMNA*. The mechanism by which a mutation in *LMNA* alters nuclear function and causes disease remains unclear. So far, only two publications have described ultrastructural and immunochemical changes associated with *LMNA* defects in DCM:[5 6] (*a*) reduced *LMNA* expression in the myocyte nuclei, and (*b*) nuclear membrane damage, such as focal disruptions, blebs, and nuclear pore clustering.

In this report, we describe new mutations found through *LMNA* screening in our DCM population. We determined the effect of *LMNA* mutations in heart tissue obtained from two patients carrying these novel mutations. In order to understand the cellular mechanisms leading to the observed cardiac phenotypes, we expressed *LMNA* mutations in a cellular model and performed live cell analysis. We found that overexpression of a specific mutated lamin C influences the spatial organisation of lamin intranuclear speckles. Previous studies have suggested a role for these speckles in controlling gene expression.[7] We show here that an *LMNA* mutation is able to disrupt the normal nucleoplasmic distribution of the small ubiquitin-like modifier 1 (SUMO1), which is emerging as a major regulatory protein involved in chromatin organisation and gene expression.[8]

## METHODS

### Subjects, heart tissues, and *LMNA* screening

Written informed consent was obtained from 92 DCM probands and their relatives in accordance with study protocols approved by hospital ethics committees.

Each amplified DNA fragment from *LMNA* was submitted to both single strand conformational polymorphism electrophoresis[9] and denaturing high performance liquid chromatography (DHPLC) (Helix, Varian) analysis.

Detailed descriptions of patient and family recruitment, heart tissue collection and processing, and screening methods are provided as supplementary online information at http://jmg.bmjjournals.com/supplemental/.

### Construction of expression plasmids

Full length lamin C cDNA was obtained by PCR amplification of first strand cDNAs (forward primer 5′-GGAATTCCATGGAGACCCCGTCCCAGCG-3′, reverse primer 5′-GCGGATCCTCAGCGGCGGCTACCACTCA-3′). The amplicon was inserted in the multiple cloning sites of both pECFP-C1 (cyan) and

**Abbreviations:** DCM, dilated cardiomyopathy; SUMO1, small ubiquitin-like modifier 1



J Med Genet: first published as 10.1136/jmg.2004.023283 on 1 August 2005. Downloaded from http://jmg.bmj.com/ on June 16, 2021 by guest. Protected by copyright.

pEYFP-C1 (yellow) vectors (Clontech Laboratories). The cDNA encoding wild type prelamin A, cloned into pcDNA4 (Invitrogen) was kindly provided by Drs Morris and Holt (North East Wales Institute, UK). The vector was transformed in XL competent *Escherichia coli*. Point mutations found in DCM patients were introduced by using the Transformer site directed mutagenesis kit (Clonetech Laboratories). SUMO1 amplified by PCR was fused to pEYFP-C3. Deletion of the five C-terminal residues in the pEYFP:SUMO1 construct was achieved by replacing glycine 97 with a stop codon. All clones were systematically sequenced.

## Cell culture and transfection

COS7 cells (ATCC) were cultured on glass coverslips in Dulbecco's modified Eagle's medium glutamax, supplemented with 10% fetal bovine serum and 1% L-glutamine. The transfection of fusion protein constructs was made using 0.5 µg of expression vectors and Lipofectamine 2000 (Life Technologies). Cells were grown for 17–21 hours. Both cyclohexamide (28 µg/ml) and Hoechst 33258 Dye (10 µg/ml) were added for 30 minutes prior to microscopic observation to halt transcription and visualise chromosomes, respectively. Excitation wavelengths were 434 nm for CFP:lamin C, 514 nm for YFP:lamin C, YFP:SUMO1, and

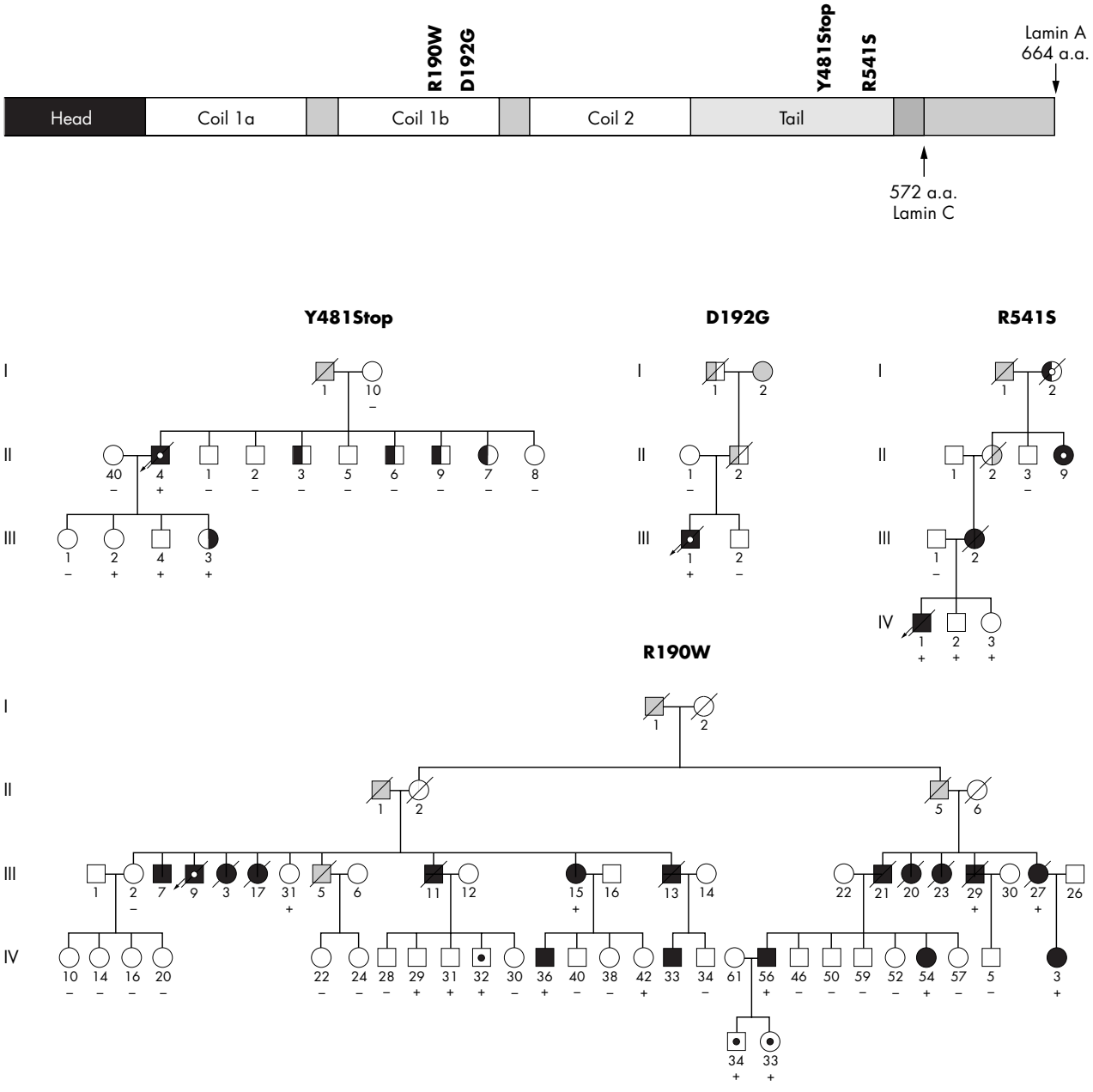


**Figure 1** Pedigree of the families with *LMNA* mutations and location of the identified mutation on a schema of *LMNA* primary sequence. Arrow indicates proband; black filled symbol, dilated cardiomyopathy; open symbol, asymptomatic; grey filled symbol, no clinical data; left half filled symbol (black), left ventricular dilatation; right half filled symbol (black), right bundle branch block; left half filled symbol (grey), heart failure; right half filled symbol (grey), sudden death; black filled dot within symbol, unknown dilated cardiomyopathy status; grey filled dot within symbol, muscular dystrophy; diagonal lines, death; + or − sign, presence or absence of mutations.



J Med Genet: first published as 10.1136/jmg.2004.023283 on 1 August 2005. Downloaded from http://jmg.bmj.com/ on June 16, 2021 by guest. Protected by copyright.

YFP-SUMO1ΔC5, 350 nm for Hoechst 33258 dye, and 575 nm for secondary antibodies.

### Timelapse microscopy

Glass coverslips were mounted in live cell chambers in regular growth media supplemented with 20 mmol/l HEPES (pH 7.4), visualised at 100× magnification in an enclosed Olympus 1×70 inverted microscope, and processed using TILLvisION software (version 4.0). Videos were taken through a CFP/YFP dual pass filter (Till Photonics, 500 ms).

### Immunochemistry and immunoblotting

The primary antibodies used were lamin A/C 131C3 monoclonal antibody (Chemicon International), lamin A 133A2 monoclonal antibody (Abcam), emerin G45 monoclonal antibody (Novocastra Laboratories), and SUMO 1/Sentrin polyclonal antibody (Oncogene research product). Detailed description is provided as supplementary online information at http://jmg.bmjjournals.com/supplemental/.

## RESULTS

### *LMNA* mutations and clinical characteristics of mutations carriers

In total, 92 DCM probands were screened for variations within *LMNA* coding sequence and exon–intron boundaries. Four mutations in four unrelated DCM families were found. All mutations were located in highly conserved regions of the gene shared by lamin A and C isoforms. Expressed phenotypes in the 22 mutation carriers were highly variable between families and within families. There were 10 symptomatic mutation carriers, while four adult mutation carriers (age range 23–43 years) and four children (age range 6–14 years) were asymptomatic (clinical characteristics of *LMNA* mutation carriers are provided as supplementary online information at http://jmg.bmjjournals.com/supplemental/). Symptomatic mutation carriers were characterised by poor prognosis. In total, of 22 symptomatic family members, 5 patients received heart transplant and 12 died from DCM.

The R190W mutation (C780T transition) was found in a large family from the UK with autosomal dominant inheritance (fig 1). Clinical features for some of the family members have been detailed in a previous publication.[10] The D192G mutation (A787G transition) (GenBank accession number AY847595) was found in a Polish family with suspected autosomal dominant transmission (fig 1). The Y481stop mutation (C1656G transversion) (GenBank accession no. AY847596) was found in an unrelated Polish patient (fig 1) and the R541S mutation (C1833A transversion) (GenBank accession no. AY847597) in a Canadian family with suspected autosomal dominant transmission (fig 1).

### Pathological studies of hearts from patients with end stage DCM

Light microscopy of the two available heart samples from patients carrying D192G and R541S *LMNA* mutations revealed non-specific myocyte damage and interstitial fibrosis (data not shown). Electron micrographs of the heart tissue sections from the D192G *LMNA* patient demonstrated dramatic morphological alterations, including a complete loss of the nuclear envelope (fig 2A), the accumulation of mitochondria, glycogen and/or lipofuscin in the nucleoplasm, and chromatin disorganisation (fig 2B) in approximately 30% of nuclei. By contrast, examination of the heart tissue sections from the patient with R541S *LMNA* revealed only non-specific nuclear membrane alterations (fig 2C), comparable with those found in transplanted DCM patients without LMNA mutation (fig 2D). Immunostaining with mouse antihuman lamin A + C monoclonal antibody showed normal staining of interstitial, vascular, and myocyte nuclei for both the D192G and R541S patient hearts (fig 2E,F,G).

### Effects of overexpression of mutated *LMNA* in COS7 cell model

To characterise the consequences of *LMNA* mutations at the cellular level, transient cell transfections were performed on COS7 cells with wild type and/or mutated lamin C mRNA expressed as fusions to the C-terminus of variants of the *Aequorea victoria* green fluorescent protein (GFP) (lamin C-FP). Wild type and mutated lamin C-FP appeared to strictly colocalise with Hoechst 33258 chromosome dye in the nucleus (fig 3A). Wild type lamin C-FP formed distinct intranucleoplasmic foci in most cells. This individualisation of the intranucleolar granules in numerous discrete speckles was previously observed in Swiss 3T3 and SW13 cells,[11 12] (fig 3A). Timelapse video fluorescence microscopy indicated that the intranuclear structures were relatively stable (up to 5 hours) and showed no obvious alteration in number, shape, or location over the time period. In a few cells, we observed a smaller number of spots, which were much larger and tended to be round. During transient expression of D192G lamin C-FP, the number of cells displaying a few large fluorescent rounded spots was dramatically increased compared with wild type lamin C-FP ($p<0.0001$; fig 3A,C). Indeed, a single giant round spot was present in the nucleus of a mean (SD) 84 (6)% of cells. This spot appeared to be stable in shape and

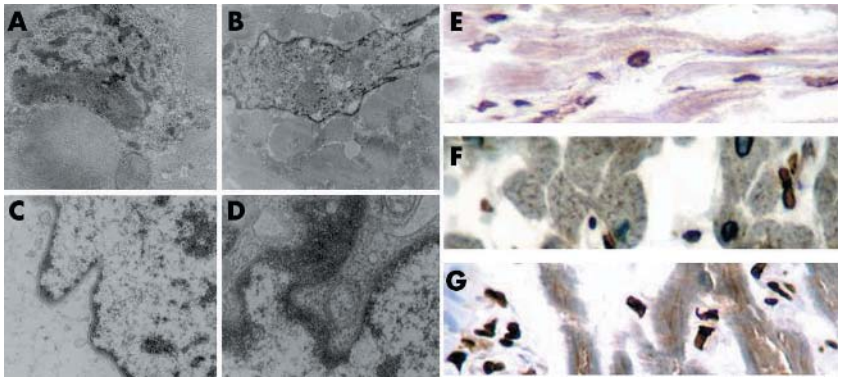


**Figure 2** (A–D) Electron micrographs of cardiomyocytes from end stage dilated cardiomyopathy patients with or without *LMNA* mutation. (A) Total loss of nuclear membrane in D192G *LMNA* patient; (B) accumulation of mitochondria and glycogen in the nucleoplasm and chromatin disorganisation in D192G *LMNA* patient; (C) non-specific alteration in R541S *LMNA* patient; (D) non-specific alteration in end stage dilated cardiomyopathy patient with wild type *LMNA*; (E–G) normal immunostaining with mouse antihuman lamin A+C monoclonal antibody in D192G, R541S, and wild type *LMNA* patients. (Original magnifications: (A) ×20 000; (B) ×12 000; (C) ×30 000; (D) ×60 000; (E–G) ×400).

J Med Genet: first published as 10.1136/jmg.2004.023283 on 1 August 2005. Downloaded from http://jmg.bmj.com/ on June 16, 2021 by guest. Protected by copyright.

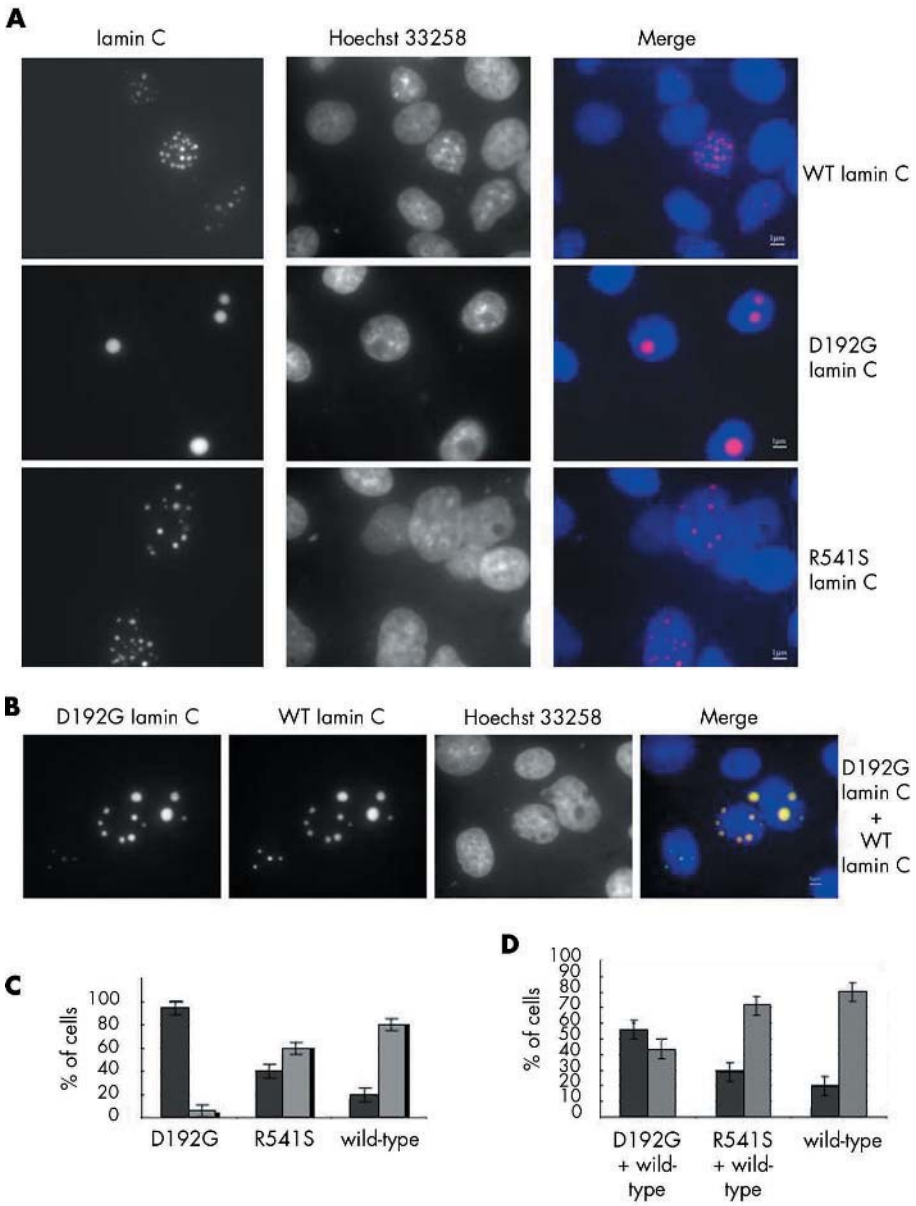


**Figure 3** (A) COS7 cells transfected with fluorescently tagged wild type (WT) lamin C, D192G lamin C, and R541S lamin C showing the location of the lamin C (red) within the nucleus visualised by Hoechst 33258 dye (blue). (B) COS7 cells co-transfected with equimolar amounts of fluorescently tagged D192G (red) and wild type lamin C (yellow green) showing their co-location within the nucleus. Ratio of fluorescence was approximately 1. (C, D). Number of spots per transfected cells or cells co-transfected with wild type and mutant lamin C. Data are presented as mean (standard error) calculated from at least three independent experiments. $\chi^2$ tests showed significant differences across genotypes ($p<0.0001$) for single transfection experiments (C). The number of spots was significantly different in cells coexpressing D192G and WT lamin C compared with cells expressing WT lamin C ($p<0.0001$), and in cells coexpressing D192G and WT lamin C compared with cells co-expressing R541S and WT lamin C ($p<0.0001$). The number of spots was not significantly different in cells co-expressing R541S and WT lamin C compared with cells expressing WT lamin C ($p>0.1$). Black bars, number of cells with <3 spots; grey bars, number of cells with >3 spots.

location within the nucleus, as indicated by overnight timelapse videos. Transfection efficiency range was 30–60%. Western blotting quantification of endogenous versus transfected lamin showed that overexpression resulted in a 2.2-fold to 15.7-fold increase, with a mean (SD) overexpression of 10.08 (6.0). However, the D192G lamin C-FP typical pattern was obvious in every experiment regardless of the transfection efficiency or the overexpression levels. Importantly, the presence of these giant spots in the D192G lamin C-FP transfected cells could not be explained by a higher rate of expression of the mutated than the wild type lamin C-FP, as the transfection ratio of mutated versus wild type was not different from 1 (1.15 (0.07)).

In order to mimic a heterozygous state, we coexpressed wild type and the D192G lamin C. Coexpression only partly restored the wild type phenotype (fig 3B), with approximately 50% of cells displaying a wild type phenotype (fig 3D). Wild type and mutated lamin C co-distributed in the nucleoplasmic foci (fig 3B). Transient expression of the R541S lamin C-FP led to an intermediate phenotype with fewer and more spherical foci than the wild type phenotype, the number of cells displaying a unique spot being about 40% (fig 3A, C). Coexpression of wild type and the R541S lamin C completely restored the wild type phenotype (fig 3D). Overexpression of the R190W and Y481stop lamin C did not result in a specific phenotype (data not shown).



J Med Genet: first published as 10.1136/jmg.2004.023283 on 1 August 2005. Downloaded from http://jmg.bmj.com/ on June 16, 2021 by guest. Protected by copyright.

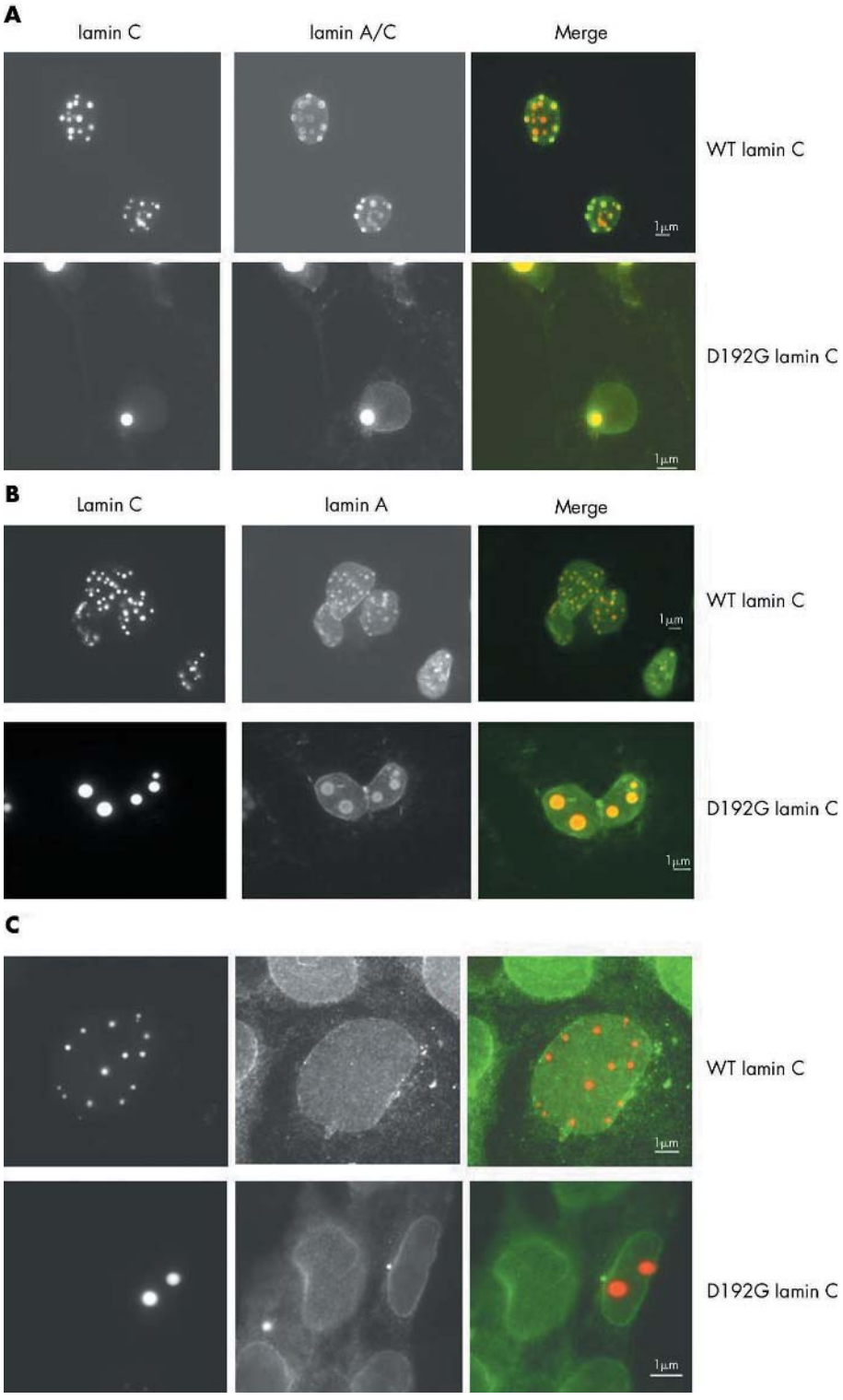


**Figure 4** COS7 Cells transfected with fluorescently tagged wild type (WT) or D192G lamin C (red) and labelled with (A) anti-lamin A/C, (B) anti-lamin A, or (C) anti-emerin antibody (yellow green) and showing that the WT or the D192G lamin C-FP foci did not disturb the distribution of endogenous lamins or emerin on the nuclear rim.

As previously reported for wild type lamin C-FP,[11–15] wild type or D192G lamin C-FP foci did not disturb the distribution of endogenous lamins or emerin on the nuclear rim as detected by immunofluorescence (fig 4A–C). However, a readily detectable fraction of the endogenous lamin is recruited at the periphery of the foci (fig 4A, B).

It has been suggested that lamin A plays a central role in tethering lamin C to the nuclear envelope.[11–13] We tested whether restoration of the stochiometry, through co-transfecting lamin A and C, leads to a relocalisation of lamin C-FP to the nuclear envelope. As shown in fig 5, co-transfection of wild type prelamin A and lamin C resulted in the redirection



J Med Genet: first published as 10.1136/jmg.2004.023283 on 1 August 2005. Downloaded from http://jmg.bmj.com/ on June 16, 2021 by guest. Protected by copyright.

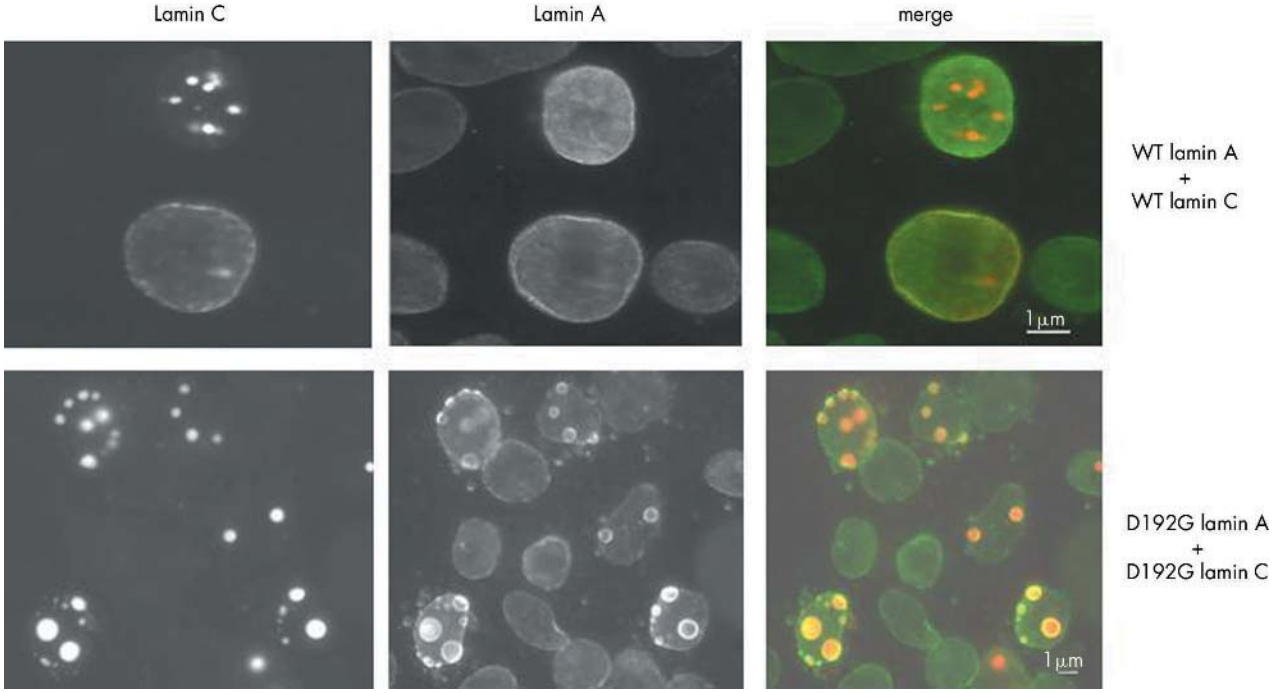


**Figure 5** COS7 Cells co-transfected with wild type (WT) prelamin A and fluorescently tagged WT lamin C (red) or D192G prelamin A and fluorescently tagged D192G lamin C (red) and labelled with anti-lamin A antibody (yellow green). The presence of WT lamin A resulted in the re-targeting of WT lamin C to the nuclear membrane. D192G lamin C speckles are surrounded by a halo of lamin A, which tends to merge with the nuclear envelope at fusion points. Fluorescently tagged D192G lamin C was not observed in the nuclear envelope.

of lamin C-FP to the nuclear envelope and the reduction of the granular aspect of the nucleoplasm in a significant proportion of the cells. By contrast, this phenomenon was never observed when both the D192G prelamin A and D192G lamin C were co-transfected (fig 5). The D192G lamin C speckles surrounded by the D192G lamin A tend to merge with the nuclear envelope at fusion points where an enrichment of lamin A was observed. However, the D192G lamin C was never identified in the lamina.

### Effect of the D192G *LMNA* mutation on SUMO1 distribution pattern

Previous studies have proposed a role for internal lamin speckles in controlling gene expression and demonstrated that the reorganisation of lamin speckles into enlarged foci is correlated to inhibition of transcription.[7] As major cell regulatory systems targeted by sumoylation are regulation of chromatin organisation and gene expression,[8] we determined whether the normal distribution of SUMO1 was conserved in the presence of mutated lamin C. To this end, we co-expressed wild type or mutated lamin C and SUMO1 or SUMO1ΔC5 in COS7 cells. Western blotting quantification of endogenous versus transfected SUMO1 showed that the overexpression was around fivefold. SUMO1ΔC5 is a mutant form of SUMO1 lacking the C-terminal diglycine motif that is essential for covalent modification by SUMO1.[16] As shown in fig 6A, SUMO1:FP was normally distributed in cell nucleus.[17] When SUMO1-FP was co-transfected with the D192G lamin C-FP, SUMO1-FP appeared to be recruited and to concentrate in the middle of giant rounded lamin C spots (fig 6A). Co-expression of SUMO1-FP and R541S lamin C-FP resulted in a phenotype indistinguishable from the wild type phenotype (data not shown). By contrast, the SUMO1ΔC5-FP pattern remained diffuse in presence of both wild type and mutated lamin C (fig 6B). Therefore, the specificity of the dot-like staining of SUMO1-FP in the presence of the D192G lamin C seemed to be dependent on the sumoylation function of SUMO1.

## DISCUSSION

By screening DNA from 92 DCM probands, we found four mutations confirming that *LMNA* mutations occur in a significant proportion (4%) of DCM patients. Although it has been suggested[18] that *LMNA* mutation carriers with symptomatic DCM are characterised by poor prognosis, more than 18% of the adult carrier population we studied was unaffected. While the R190W *LMNA* mutation was previously reported in two related patients in their forties with DCM associated with conduction system defect,[5] and in four related patients including one with isolated left ventricular noncompaction,[19] to our knowledge the D192G, Y481stop and R541S mutations have not been reported elsewhere. However, an Y481H *LMNA* mutation was found to be associated with autosomal dominant limb girdle muscular dystrophy with cardiac conduction block.[20] Mutations in the Arg541 codon were reported to be associated with both Emery-Dreifuss muscular dystrophy (R541H)[20] and DCM with conduction defects (R541C).[21] Altogether, these results confirm that, despite DCM being considered a monogenic disorder, additional genetic and/or environmental factors contribute to the clinical phenotype.

Previous studies have reported nuclear membrane damage, such as focal disruptions, blebs, and nuclear pore clustering in myocytes from DCM patients with *LMNA* mutations.[5 6] Similar morphological alterations of the nuclear membrane have been reported in different tissues from *LMNA* mutation carriers who are affected by other diseases,[22–24] and in animal models.[25–27] Based on these findings, it was postulated that the cardiomyocytes from the two end stage DCM patients carrying *LMNA* mutations would also demonstrate indications of nuclear membrane damage. Surprisingly, while heart tissue sections from the D192G *LMNA* carrier revealed



J Med Genet: first published as 10.1136/jmg.2004.023283 on 1 August 2005. Downloaded from http://jmg.bmj.com/ on June 16, 2021 by guest. Protected by copyright.

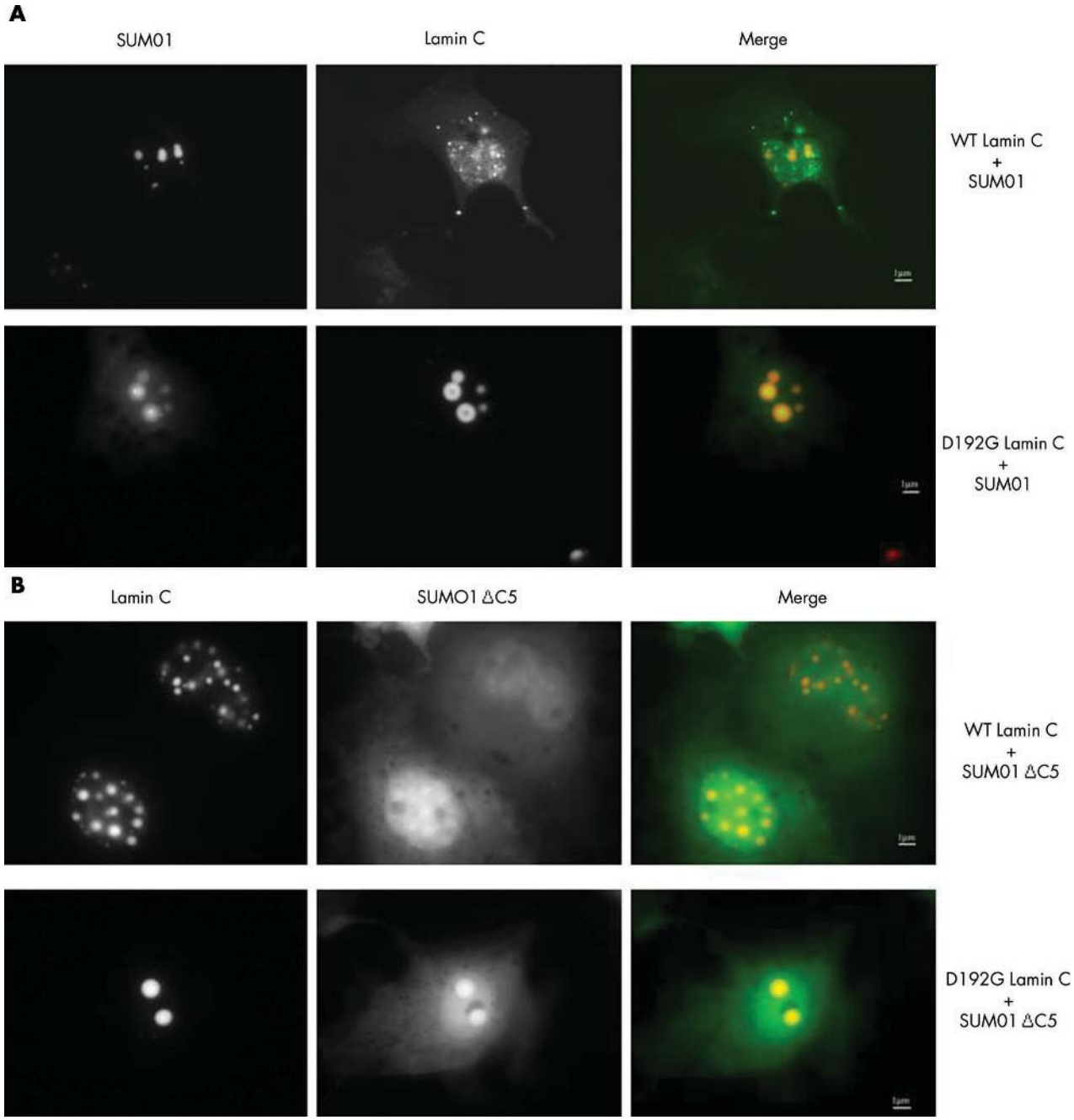


**Figure 6** COS7 Cells co-transfected with fluorescently tagged lamin C (red) and (A) SUMO1 or (B) SUMO1ΔC5 (yellow green). (A) Presence of wild type lamin C did not alter SUMO1 distribution (small dots within and nearby the nucleus), while co-transfection with D192G lamin C shows recruitment of SUMO1 within the lamin C spots. (B) No difference is observed in the localisation of SUMO1ΔC5 in cell transfected with wild type lamin C or D192G lamin.

marked nuclear abnormalities, cardiomyocytes from the patient carrying the R541S mutation presented only modest and non-specific nuclear membrane alterations. It is clear from these observations that direct correlations between any of the morphological changes and the mutations cannot be made.

In order to unravel the observed cardiac phenotypes, we expressed *LMNA* mutations in a cellular model and performed live cell analysis. While both phenotypes induced by overexpression of the R190W and Y481stop were indistinguishable from the wild type, overexpression of the D192G lamin C induced a reorganisation of the lamin speckles into a unique and giant round spot in the vast majority of cells, despite expression level of the D192G lamin C being similar to the wild type. When the R541S lamin C was expressed, the phenotype was intermediate with fewer spherical foci than the wild type phenotype. *LMNA* mutations resulting in punctuate distribution across the nuclear surface of lamin A and C have been previously reported in vitro,[28 29] and in patient fibroblasts.[14 30]

To mimic a heterozygous state, we co-transfected the mutated lamin C with the wild type, and demonstrated that the rearrangement of lamin speckles was partially (D192G) or fully (R541S) reversed. The rescue of the wild type phenotype for R541S may explain why the patient carrying the R541S heterozygous mutation displays non-specific



J Med Genet: first published as 10.1136/jmg.2004.023283 on 1 August 2005. Downloaded from http://jmg.bmj.com/ on June 16, 2021 by guest. Protected by copyright.

cardiac ultrastructural changes. It cannot be excluded that this patient carries a mutation in another DCM gene. By contrast, the discrete giant lamin speckles seen with the D192G lamin C persisted even in the presence of D192G lamin A, suggesting that those mutants are assembly incompetent. The lamin A tended to form a halo around the D192G lamin C speckles, which merged with the nuclear envelope at lamin A enrichment points. This lamin A halo was previously observed when cells were transfected with the N195K, E358K, and M371K mutant lamin A alone;[29] here we show that the mutant lamin C is trapped inside. As a consequence of compromised lamina integrity observed in vitro, the nuclear envelope may become more fragile. This may result in the ultrastructural damage of the nuclear envelope, including the loss of the nuclear membrane in the heart tissue of patients carrying such mutations.

Synchronous and reversible formation of enlarged and rounded foci of lamin A/C have been described following the inhibition of transcription.[7] Conversely, disruption of lamin speckles leads to a downregulation of the transcription.[7] It was speculated that lamin speckles are part of a dynamic structure that can be rapidly modulated by specific signalling events to spatially organise RNA polymerase II transcription.[7] Given these data and our results, the speckle formation induced by mutated lamin A/C may result in ''freezing'' of the cells in a transient and/or a pathological phase that corresponds to a deregulated transcription state.

In vitro and in vivo interactions between A-type lamins and transcription factors have been reported.[31 32] In lamin A/C deficient mice that develop DCM, alterations in nuclear architecture are associated with reduced PPARγ expression, a lack of hypertrophic gene activation, and decreased SREBP1 (sterol response element binding protein 1) import via nuclear pores.[33] On the other hand, lamins A/C have been suggested to anchor (*a*) chromatin, through BAF, which can bind directly to DNA,[34] and (*b*) nuclear pores by means of their binding to NUP153.[35] Clustering of nuclear pores has been frequently reported in patients with *LMNA* mutations.[5 6 36] Given those observations, we hypothesised that the effect of *LMNA* mutations might be mediated by the interference of mutated lamin with the SUMO1 pathway. Indeed, reversible covalent modification of proteins with SUMO1 is emerging as an important system contributing primarily to regulation of gene expression and chromatin organisation.[8] RNA polymerase II was shown to be sumoylated in human embryonic kidney-293 (HEK-293) cells.[8] Furthermore, enzymes involved in the SUMO modification process are components of the nuclear pore complex.[37] SENP2, a SUMO cleaving protease, interacts with the FG repeat domain of NUP153, the nucleoporin that interacts with the lamins.[35 37] When SUMO1 was co-transfected with the D192G lamin C in COS7 cells, all SUMO1 conjugated proteins appeared to be recruited and trapped in the middle of giant lamin C spots. Moreover, this abnormal pattern of distribution is dependent on the sumoylation function of SUMO1. As the formation of type A lamin foci was reported for multiple *LMNA* mutations both in vitro,[28 29] and in patient fibroblasts,[14 30] this new mechanism by which mutated type A lamin might exert their effects may be common to those mutations. Mutations leading to speckle formation are located all along the *LMNA* gene and are predicted to modify several amino acids from position 85 to position 530.[14 28–30] Those mutations were linked to DCM, autosomal dominant Emery-Dreifuss muscular dystrophy, as well as Dunnigan-type familial lipodystrophy.[14 28–30] By abolishing or reducing the availability of the sumoylated protein pool in the nucleus, those mutations may disturb functions controlled by sumoylation.

In conclusion, we showed an absence of specific phenotype for the R541S *LMNA* mutation both in vivo and in vitro. These findings question the supposition that the R541S *LMNA* mutation is the primary genetic defect responsible for the development of heart failure in such patients and therefore, raises concerns regarding the reliability of genetic counselling to patients and their families. By contrast, the D192G *LMNA* mutation is associated in vivo with dramatic morphological changes of the cardiomyocyte nucleus and in vitro with total disorganisation of type A lamins; this lamin mutant trapped SUMO1 modified proteins presented in the nucleus. Therefore, our hypothesis is that *LMNA* mutants leading to the formation of intranuclear speckles induce not only nuclear envelope structural damage, but also the deregulation of cellular functions controlled by sumoylation, such as transcription, chromosome organisation, and protein and RNA nuclear trafficking.

## ACKNOWLEDGEMENTS

These studies would not have been possible without the invaluable assistance of patients and family members. We wish to thank P Rippstein and W Parks (Ottawa Hospital Department of Pathology) for their excellent histological technical assistance, and from the University of Ottawa Heart Institute, R Brown for his helpful technical advice, K Williams for her assistance with statistical calculations, R Zunino for his excellent technical assistance, and K Adamo for her critical review of the manuscript. We also thank Drs G E Morris and I Holt (North East Wales Institute, UK) for the gift of prelamin A cDNA.

Supplementary information can be viewed on the *JMG* website at http://www.jmedgenet.com/supplemental.

**Authors' affiliations**

**N Sylvius, P M Bolongo, S Poon, F Tesson,** Laboratory of Genetics of Cardiac Diseases, University of Ottawa Heart Institute, Ottawa, ON, Canada
**Z T Bilinska, J Grzybowski, W Ruzyllo,** National Institute of Cardiology, Warsaw, Poland
**J P Veinot,** Department of Pathology and Laboratory Medicine, University of Ottawa, Anatomical Pathology, Ottawa Hospital, Ottawa, ON, Canada
**A Fidzianska,** Polish Academy of Sciences, Warsaw, Poland
**P McKeown,** Department of Medicine, Queen's University of Belfast, Belfast, UK
**R A Davies, K-L Chan, A S L Tang,** Division of Cardiology, University of Ottawa Heart Institute, Ottawa, ON, Canada
**S Dyack,** Department of Pediatrics, Dalhousie University, Halifax, NS, Canada
**H McBride,** Lipoproteins and Atherosclerosis Unit, University of Ottawa Heart Institute, Ottawa, ON, Canada

This research was supported by Canadian Institutes for Health Research operating grants 38054 and 65152, and by Heart and Stroke Foundation grant NA 5101 awarded to F Tesson. Polish patients and families were studied with support of grant no. 0010/P05B/98/14 from the Polish Committee for Scientific Research. N Sylvius is the recipient of the fellowship awarded by the Heart and Stroke Foundation of Ontario Program grant 5275.

Competing interests: none declared

## REFERENCES

1 **Mangin L**, Charron P, Tesson F, Mallet A, Dubourg O, Desnos M, Benaische A, Gayet C, Gibelin P, Davy JM, Bonnet J, Sidi D, Schwartz K, Komajda M. Familial dilated cardiomyopathy: clinical features in French families. *Eur J Heart Fail* 1999;**1**:353–61.
2 **Mestroni L**, Rocco C, Gregori D, Sinagra G, Di Lenarda A, Miocic S, Vatta M, Pinamonti B, Muntoni F, Caforio AL, McKenna WJ, Falaschi A, Giacca M, Camerini. Familial dilated cardiomyopathy: evidence for genetic and phenotypic heterogeneity. Heart Muscle Disease Study Group. *J Am Coll Cardiol* 1999;**34**:181–90.



J Med Genet: first published as 10.1136/jmg.2004.023283 on 1 August 2005. Downloaded from http://jmg.bmj.com/ on June 16, 2021 by guest. Protected by copyright.

3 **Sylvius N**, Tesson F, Gayet C, Charron P, Benaiche A, Peuchmaurd M, Duboscq-Bidot L, Feingold J, Beckmann JS, Bouchier C, Komajda M. A new locus for autosomal dominant dilated cardiomyopathy identified on chromosome 6q12–q16. *Am J Hum Genet* 2001;**68**:241–6.
4 **Navarro CL**, De Sandre-Giovannoli A, Bernard R, Boccaccio I, Boyer A, Genevieve D, Hadj-Rabia S, Gaudy-Marqueste C, Smitt HS, Vabres P, Faivre L, Verloes A, Van Essen T, Flori E, Hennekam R, Beemer FA, Laurent N, Le Merrer M, Cau P, Levy N. Lamin A and ZMPSTE24 (FACE-1) defects cause nuclear disorganization and identify restrictive dermopathy as a lethal neonatal laminopathy. *Hum Mol Genet* 2004;**13**:2493–503.
5 **Arbustini E**, Pilotto A, Repetto A, Grasso M, Negri A, Diegoli M, Campana C, Scelsi L, Baldini E, Gavazzi A, Tavazzi L. Autosomal dominant dilated cardiomyopathy with atrioventricular block: a lamin A/C defect-related disease. *J Am Coll Cardiol* 2002;**39**:981–90.
6 **Verga L**, Concardi M, Pilotto A, Bellini O, Pasotti M, Repetto A, Tavazzi L, Arbustini E. Loss of lamin A/C expression revealed by immuno-electron microscopy in dilated cardiomyopathy with atrioventricular block caused by LMNA gene defects. *Virchows Arch* 2003;**443**:664–71.
7 **Kumaran RI**, Muralikrishna B, Parnaik VK. Lamin A/C speckles mediate spatial organization of splicing factor compartments and RNA polymerase II transcription. *J Cell Biol* 2002;**159**:783–93.
8 **Zhao Y**, Kwon SW, Anselmo A, Kaur K, White MA. Broad spectrum identification of cellular small ubiquitin-related modifier (SUMO) substrate proteins. *J Biol Chem* 2004;**279**:20999–1002.
9 **Tesson F**, Sylvius N, Pilotto A, Dubosq-Bidot L, Peuchmaurd M, Bouchier C, Benaiche A, Mangin L, Charron P, Gavazzi A, Tavazzi L, Arbustini E, Komajda M. Epidemiology of desmin and cardiac actin gene mutations in a european population of dilated cardiomyopathy. *Eur Heart J* 2000;**21**:1872–6.
10 **MacLennan BA**, Tsoi EY, Maguire C, Adgey AA. Familial idiopathic congestive cardiomyopathy in three generations: a family study with eight affected members. *Q J Med* 1987;**63**:335–47.
11 **Pugh GE**, Coates PJ, Lane EB, Raymond Y, Quinlan RA. Distinct nuclear assembly pathways for lamins A and C lead to their increase during quiescence in Swiss 3T3 cells. *J Cell Sci* 1997;**110**:2483–93.
12 **Vaughan A**, Alvarez-Reyes M, Bridger JM, Broers JL, Ramaekers FC, Wehnert M, Morris GE, Whitfield WGF, Hutchison CJ. Both emerin and lamin C depend on lamin A for localization at the nuclear envelope. *J Cell Sci* 2001;**114**:2577–90.
13 **Muralikrishna B**, Dhawan J, Rangaraj N, Parnaik VK. Distinct changes in intranuclear lamin A/C organization during myoblast differentiation. *J Cell Sci* 2001;**114**:4001–11.
14 **Muchir A**, Medioni J, Laluc M, Massart C, Arimura T, van der Kooi AJ, Desguerre I, Mayer M, Ferrer X, Briault S, Hirano M, Worman HJ, Mallet A, Wehnert M, Schwartz K, Bonne G. Nuclear envelope alterations in fibroblasts from patients with muscular dystrophy, cardiomyopathy, and partial lipodystrophy carrying lamin A/C gene mutations. *Muscle Nerve* 2004;**30**:444–50.
15 **Reichart B**, Klafke R, Dreger C, Kruger E, Motsch I, Ewald A, Schafer J, Reichmann H, Muller CR, Dabauvalle MC. Expression and localization of nuclear proteins in autosomal-dominant Emery-Dreifuss muscular dystrophy with LMNA R377H mutation. *BMC Cell Biol* 2004;**5**:12.
16 **Johnson ES**, Schwienhorst I, Dohmen RJ, Blobel G. The ubiquitin-like protein Smt3p is activated for conjugation to other proteins by an Aos1p/Uba2p heterodimer. *EMBO J* 1997;**16**:5509–19.
17 **Saitoh H**, Hinchey J. Functional heterogeneity of small ubiquitin-related protein modifiers SUMO-1 versus SUMO-2/3. *J Biol Chem* 2000;**275**:6252–8.
18 **Taylor MR**, Fain PR, Sinagra G, Robinson ML, Robertson AD, Carniel E, Di Lenarda A, Bohlmeyer TJ, Ferguson DA, Brodsky GL, Boucek MM, Lascor J, Moss AC, Li WL, Stetler GL, Muntoni F, Bristow MR, Mestroni L. Natural history of dilated cardiomyopathy due to lamin A/C gene mutations. *J Am Coll Cardiol* 2003;**41**:771–80.
19 **Hermida-Prieto M**, Monserrat L, Castro-Beiras A, Laredo R, Soler R, Peteiro J, Rodriguez E, Bouzas B, Alvarez N, Muniz J, Crespo-Leiro M. Familial dilated cardiomyopathy and isolated left ventricular noncompaction associated with lamin A/C gene mutations. *Am J Cardiol* 2004;**94**:50–4.
20 **Kitaguchi T**, Matsubara S, Sato M, Miyamoto K, Hirai S, Schwartz K, Bonne G. A missense mutation in the exon 8 of lamin A/C gene in a Japanese case of autosomal dominant limb-girdle muscular dystrophy and cardiac conduction block. *Neuromuscul Disord* 2001;**11**:542–6.
21 **Forissier JF**, Bonne G, Bouchier C, Duboscq-Bidot L, Richard P, Wisnewski C, Briault S, Moraine C, Dubourg O, Schwartz K, Komajda M. Apical left ventricular aneurysm without atrio-ventricular block due to a lamin A/C gene mutation. *Eur J Heart Fail* 2003;**5**:821–5.
22 **Fidzianska A**, Toniolo D, Hausmanowa-Petrusewicz I. Ultrastructural abnormality of sarcolemmal nuclei in Emery-Dreifuss muscular dystrophy (EDMD). *J Neurol Sci* 1998;**159**:88–93.
23 **Vigouroux C**, Auclair M, Dubosclard E, Pouchelet M, Capeau J, Courvalin JC, Buendia B. Nuclear envelope disorganization in fibroblasts from lipodystrophic patients with heterozygous R482Q/W mutations in the lamin A/C gene. *J Cell Sci* 2001;**114**:4459–68.
24 **Novelli G**, Muchir A, Sangiuolo F, Helbling-Leclerc A, D'Apice MR, Massart C, Capon F, Sbraccia P, Federici M, Lauro R, Tudisco C, Pallotta R, Scarano G, Dallapiccola B, Merlini L, Bonne G. Mandibuloacral dysplasia is caused by a mutation in LMNA-encoding lamin A/C. *Am J Hum Genet* 2002;**71**:426–31.
25 **Lenz-Bohme B**, Wismar J, Fuchs S, Reifegerste R, Buchner E, Betz H, Schmitt B. Insertional mutation of the Drosophila nuclear lamin Dm0 gene results in defective nuclear envelopes, clustering of nuclear pore complexes, and accumulation of annulate lamellae. *J Cell Biol* 1997;**137**:1001–16.
26 **Sullivan T**, Escalante-Alcalde D, Bhatt H, Anver M, Bhat N, Nagashima K, Stewart CL, Burke B. Loss of A-type lamin expression compromises nuclear envelope integrity leading to muscular dystrophy. *J Cell Biol* 1999;**147**:913–20.
27 **Mounkes LC**, Kozlov S, Hernandez L, Sullivan T, Stewart CL. A progeroid syndrome in mice is caused by defects in A-type lamins. *Nature* 2003;**423**:298–301.
28 **Raharjo WH**, Enarson P, Sullivan T, Stewart CL, Burke B. Nuclear envelope defects associated with LMNA mutations cause dilated cardiomyopathy and Emery-Dreifuss muscular dystrophy. *J Cell Sci* 2001;**114**:4447–57.
29 **Ostlund C**, Bonne G, Schwartz K, Worman HJ. Properties of lamin A mutants found in Emery-Dreifuss muscular dystrophy, cardiomyopathy and Dunnigan-type partial lipodystrophy. *J Cell Sci* 2001;**114**:4435–45.
30 **Capanni C**, Cenni V, Mattioli E, Sabatelli P, Ognibene A, Columbaro M, Parnaik VK, Wehnert M, Maraldi NM, Squarzoni S, Lattanzi G. Failure of lamin A/C to functionally assemble in R482L mutated familial partial lipodystrophy fibroblasts: altered intermolecular interaction with emerin and implications for gene transcription. *Exp Cell Res* 2003;**291**:122–34.
31 **Dreuillet C**, Tillit J, Kress M, Ernoult-Lange M. In vivo and in vitro interaction between human transcription factor MOK2 and nuclear lamin A/C. *Nucleic Acids Res* 2002;**30**:4634–42.
32 **Lloyd DJ**, Trembath RC, Shackleton S. A novel interaction between lamin A and SREBP1: implications for partial lipodystrophy and other laminopathies. *Hum Mol Genet* 2002;**11**:769–77.
33 **Nikolova V**, Leimena C, McMahon AC, Tan JC, Chandar S, Jogia D, Kesteven SH, Michalicek J, Otway R, Verheyen F, Rainer S, Stewart CL, Martin D, Feneley MP, Fatkin D. Defects in nuclear structure and function promote dilated cardiomyopathy in lamin A/C-deficient mice. *J Clin Invest* 2004;**113**:357–69.
34 **Goldman RD**, Gruenbaum Y, Moir RD, Shumaker DK, Spann TP. Nuclear lamins: building blocks of nuclear architecture. *Genes Dev* 2002;**16**:533–47.
35 **Smythe C**, Jenkins HE, Hutchison CJ. Incorporation of the nuclear pore basket protein nup153 into nuclear pore structures is dependent upon lamina assembly: evidence from cell-free extracts of Xenopus eggs. *EMBO J* 2000;**19**:3918–31.
36 **Goldman RD**, Shumaker DK, Erdos MR, Eriksson M, Goldman AE, Gordon LB, Gruenbaum Y, Khuon S, Mendez M, Varga R, Collins FS. Accumulation of mutant lamin A causes progressive changes in nuclear architecture in Hutchinson-Gilford progeria syndrome. *Proc Natl Acad Sci USA* 2004;**10**:8963–8.
37 **Zhang H**, Saitoh H, Matunis MJ. Enzymes of the SUMO modification pathway localize to filaments of the nuclear pore complex. *Mol Cell Biol* 2002;**22**:6498–508.


J Med Genet: first published as 10.1136/jmg.2004.023283 on 1 August 2005. Downloaded from http://jmg.bmj.com/ on June 16, 2021 by guest. Protected by copyright.

## METHODS

### Patient and family Recruitment

The assessment of idiopathic DCM was based on diagnostic criteria, delineated by the WHO/ISFC and modified according to Mestroni and colleagues, [38].

### Heart Tissue Collection

Following written informed consent, samples were taken from right ventricle endomyocardial biopsies or from the four chambers of explanted hearts of 14 DCM patients. They were immediately processed as follows: i) for routine microscopy a portion was processed in 10 % neutral buffered formalin followed by paraffin embedding. Blocks of 5 micron thickness were sectioned and stained with hematoxylin and eosin, and if necessary, with Masson trichrome and PAS with and without diastase, ii) for electron microscopy, samples were processed in 1.6-3 % gluteraldehyde and, iii) for immunohistochemistry, samples were immediately snap-frozen in liquid nitrogen and stored at -80 °C until utilization.

### Electron microscopy

Fixed heart tissues were processed into thick and thin sections, according to standard methods. Tissue sections were examined with a Hitachi 7100 electron microscope or a JEM XII electron microscope.

### Immunochemistry

Heart tissue sample immunochemistry was done by detection of the primary antibody with a biotinylated secondary antibody followed by streptavidin-biotin-peroxidase conjugate (Quick kit-Vector Lab).

Transfected cells were fixed on coverslips with 4% paraformaldehyde in phosphate buffered saline (PBS) and permeabilized in cold acetone. Cells were incubated with the primary antibody in PBS (1:100 for the lamin A/C and the lamin A antibodies, 1:10 for the emerin antibody, and 1:200 for the SUMO1 antibody) and with Alex Fluor 594 labeled Goat Anti-Rabbit or anti-Mouse antibody (Molecular Probes) for 30 minutes. The coverslips were mounted on a glass slide with mowiol.

**Immunoblotting**

Sixteen hours after transfection, COS 7 cells were harvested and lysed in 5 ml of lysis buffer (150 mM NaCl, 2 mM $MgCl_2$, 1 mM DTT, 1% Triton-100, pH 7.4) containing a protease inhibitor cocktail, in presence or in absence of 20 mM N-ethylmaleimide. Proteins were loaded on 4-20 % Novex Tris Glycine electrophoresis gels (Invitrogen) and transferred onto nitrocellulose membranes (Bio-Rad, Hercules, CA). The primary antibodies described above were diluted in PBS/tween, 5%milk at 1:500 dilution for lamin A/C antibody, and 1:1,000 for SUMO1 antibody. The secondary antibodies were Peroxidase-linked anti-Mouse (NA931V) and anti-Rabbit (NA934V) antibodies (Amersham Bioscience). Membranes were revealed using the Western Blotting Detection reagent (ECL, Amersham Biosciences). X-Ray films were scanned using Agfa FotoLook version 3.50.01 software. The pictures were saved as TIFF files and the

quantification of the relative amount of proteins was estimated using Quantity One version 4.1.0 software (BioRad).

### *LMNA* coding sequence screening

Genomic DNA was prepared from white blood cells. Intronic oligonucleotide primers flanking each of the twelve *LMNA* exons were designed based on published sequences (Genbank accession number: L123399, L12400, and L12401). DHPLC runs were performed as recommended by Varian. Half of each PCR product was mixed with an equal amount of a previously sequenced and confirmed wild-type DNA. Mixed and unmixed samples were then denatured at 95$^{o}$C for 3 min and re-annealed by decreasing the temperature from 95$^{o}$C to 65$^{o}$C at a rate of 1$^{o}$C /min. The chosen temperatures correspond to the point at which the retention time was 75% of ($t_{rmax}$ - $t_{rmin}$). All PCR samples displaying aberrant SSCP and/or DHPLC profiles compared to wild-type controls were double-strand sequenced (ABI Prism Big Dye, AppliedBiosystems automatic sequencer). If the DNA alteration caused a non-silent variation, at least 200 control chromosomes were tested. In the case of a familial disease, the co-segregation of the potential mutation and the disease was systematically checked.

38. Mestroni L, Maisch B, McKenna WJ, Schwartz K, Charron P, Rocco C, Tesson F, Richter A, Wilke A, Komajda M. Guidelines for the study of familial dilated cardiomyopathies. Collaborative Research Group of the European Human and Capital Mobility Project on Familial Dilated Cardiomyopathy. *Eur Heart J* 1999;**20**(2):93-102.

**Table 1. Clinical Characteristics of *LMNA* Mutation Carriers.**

| Mutation | Subject | Sex/Age (years) | NYHA Class | ECG | Echocardiography | Muscular Disease | Clinical Status |
|---|---|---|---|---|---|---|---|
| R190W | III-15 | F/45 | IV | Left atrial enlargement, poor R wave progression across anterior leads, small voltages in standard leads, non-specific ST/T wave changes | LV dilatation, LVEF30% | No | Affected, Transplanted at 48 |
| R190W | III-27 | F/40 | NA | NA | NA | No | Affected, died |
| R190W | III-29 | M/40 | NA | NA | NA | No | Affected, transplanted, died |
| R190W | III-31 | F/43 | I | Normal | Normal | No | Non-Affected |
| R190W | IV-3 | F/31 | IV | NA | Moderate LV dilatation, LV dysfunction | No | Affected |
| R190W | IV-29 | M/33 | I | T wave flattening lateral leads | Normal | No | Non-Affected |
| R190W | IV-31 | M/29 | I | Wolff-Parkinson-White | Normal | No | Non-Affected |
| R190W | IV-32 | M/25 | I | Normal | Mild LV dilatation, LVEF62% | No | Uncertain |
| R190W | IV-36 | M/40 | I | T wave inversion inferior leads, non-sustained VT | Mild LV dilatation, LVEF48% | No | Affected |
| R190W | IV-42 | F/23 | I | Normal | Normal | No | Non-Affected |
| R190W | IV-54 | F/31 | II | Normal | Mild LV dilatation, LVEF40% | No | Affected |

| | | | | | | | |
|---|---|---|---|---|---|---|---|
| R190W | IV-56 | M/24 | I | Poor R wave progression anterior leads | Marked LV dilatation, Moderate LV impairment | No | Affected |
| R190W | V-33 | F/4 | I | NA | NA | NA | Uncertain |
| R190W | V-34 | M/2 | I | NA | NA | NA | Uncertain |
| D192G | III-1 | M/26 | IV | $I^{st}$ degree AVB (PR=220ms) LAFB | LVEDD60mm LVEF20% | No | Affected, died at 27 |
| Y481Stop | II-4 | M/36 | II | SVT, II degree AVB, Pacemaker | LVEDD60mm, LVEF40% | No | Affected, Transplanted at 40 |
| | | M/40 | IV | Pacemaker | LVEDD68mm LVEF20% | | |
| Y481Stop | III-2 | F/14 | I | NA | Normal | No | Non-Affected |
| Y481Stop | III-3 | F/11 | I | Incomplete RBBB | Normal | No | Uncertain |
| Y481Stop | III-4 | M/6 | I | NA | Normal | No | Non-Affected |
| R541S | III-1 | M/13 | IV | LVEDD64mm LVEF12% | Sinus tachycardia 133 bpm, diffusely low voltages, QS pattern in precordial leads, Occasional PVCs. | Epicardial fibrosis | Affected, Transplanted at 13 |
| R541S | III-2 | M/9 | I | Normal | Normal | Elevated CPK | Non-Affected |
| R541S | III-3 | F/8 | I | Normal | Normal | Elevated CPK | Non-Affected |

* Age at clinical evaluation

AVB, atrioventricular block; CPK, serum creatine-phosphokinase; LAFB, left anterior fascicular block; LV, left ventricle; LVEF, LV ejection fraction; LVEDD, LV end diastolic diameter; NA, non available; RBBB, right bundle branch block; SVT, supraventricular tachycardia